

CapeLLM: Support-Free Category-Agnostic Pose Estimation with Multimodal Large Language Models

Junho Kim
EverEx
kai@everex.co.kr

Hyungjin Chung
KAIST
EverEx
hj.chung@kaist.ac.kr

Byung-Hoon Kim*
Yonsei University
EverEx
egyptdj@yonsei.ac.kr

Abstract

Category-agnostic pose estimation (CAPE) has traditionally relied on support images with annotated keypoints, a process that is often cumbersome and may fail to fully capture the necessary correspondences across diverse object categories. Recent efforts have begun exploring the use of text-based queries, where the need for support keypoints is eliminated. However, the optimal use of textual descriptions for keypoints remains an underexplored area. In this work, we introduce **CapeLLM**, a novel approach that leverages a text-based multimodal large language model (MLLM) for CAPE. Our method only employs query image and detailed text descriptions as an input to estimate category-agnostic keypoints. We conduct extensive experiments to systematically explore the design space of LLM-based CAPE, investigating factors such as choosing the optimal description for keypoints, neural network architectures, and training strategies. Thanks to the advanced reasoning capabilities of the pre-trained MLLM, **CapeLLM** demonstrates superior generalization and robust performance. Our approach sets a new state-of-the-art on the MP-100 benchmark in the challenging 1-shot setting, marking a significant advancement in the field of category-agnostic pose estimation.

1. Introduction

Most category-specific pose estimation concentrates on training a model to recognize keypoints of a single category, such as human [25, 30, 32], vehicle [19, 20], or animal [11, 33]. This task aims to learn from images with diverse patterns, enabling the model to possess robustness on unexpected poses and scenes not encountered during training. On the contrary, those models cannot cope with categories and keypoints which have not been met before.

To estimate keypoints of novel categories, it’s essential for a model to comprehend where the points are located fol-

*Corresponding author

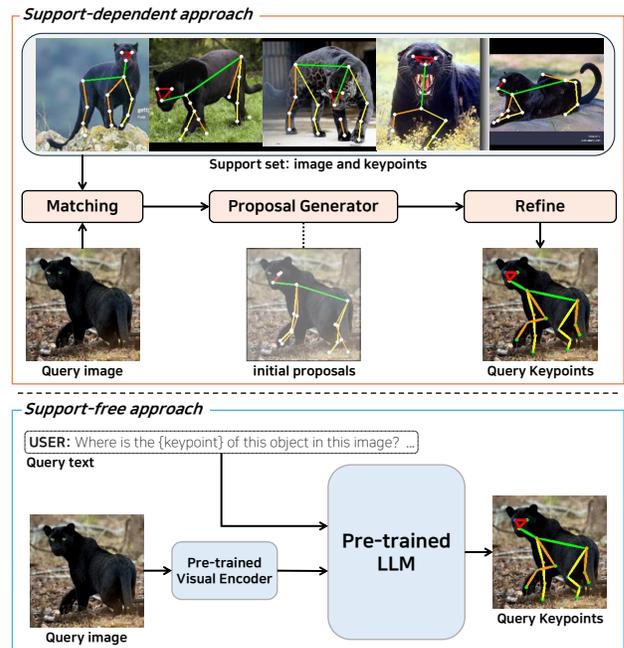


Figure 1. Architectural difference from conventional CAPE methods. Previous methods (top) are support-dependent approaches requiring support images and keypoint annotations, but ours (bottom) is one of the support-free approaches which do not need any additional images and annotations, but just text description of the keypoints

lowing additional information to figure. To this end, it is required to provide proper information about novel categories and their keypoints, allowing the model to leverage this data to deduce corresponding locations.

Category-Agnostic Pose Estimation (CAPE) tackles this issue [2, 7, 16, 21, 22, 24, 31]. It predicts keypoint positions of novel objects by employing the existing input image (called “query image”) with a set of supports. Typically, the support data comprises a pair: an image that belongs to the same category with the query but has a different pose from

it, coupled with its corresponding keypoint annotations. A prevalent technique for utilizing support data is to train the model to fuse and connect features between the query and support images [2, 7, 16, 21, 24, 31]. In the pioneering work of [31], the training was done by maximizing the similarity between the coarse features of both images. Although this method is straightforward and intuitive, it poses a high risk of overfitting to the categories used in training. To address this problem, a two-stage architecture [24] was introduced by incorporating a process to refine the similarities produced by the model, leading to a more consistent performance.

Recently, the types of support information have been diversified. A prominent example is to integrate skeletal structures—representing the connections between keypoints—into the training process as new ones. This technique not only achieves higher accuracy but also ensures robust performance against occlusions [7]. While maintaining the overall framework from previous approaches, an attempt has also been made to replace traditional support information with textual data [22]. By introducing the text-based approach, CAPE methods have gained some freedom from the inherent reliance on the supports, just replacing them with a sequence of keypoint names that are not unseen in training. Although outperforming the preceding designs [7, 24, 31] using the supports in 1-shot setting, this text-based method does not reach the 5-shot results of [7].

Employing the support information—support images and corresponding keypoint annotations—comes with inherent drawbacks. Since this method aligns support and query images that differ in many aspects aside from belonging to the same category, inadequate generalization during training can cause the model’s performance to vary depending on the quality of the support data, even with the same query image. Additionally, because keypoint information in the support is based on human annotations, it is inconvenient to update annotations whenever keypoints are modified. Even if the method [22] that uses an image with text as input seems to overcome those limitations, a structural dependency utilizing skeletal representations still exists, suggesting that a new approach that is simple yet yields reliable outputs is necessary.

Here, we aim to address this issue by utilizing a Multi-modal Large Language Model (MLLM). An MLLM [14, 27, 29] is based on a language model trained on vast amounts of multimodal data. Fully employing the Large Language Model’s (LLM’s) capability to comprehend texts, it generates the intended outputs, such as bounding boxes [27–29], masks [12]. Referring to the result that detailed descriptions make the model be improved [14] and the limitation of contrastive-learning methods in long sequences [34], we argue that it is desirable to reason keypoints of novel categories by adopting an instruction which

has detailed information about them as an input and process it by exploiting the capability of LLMs serving trustworthy results [14].

Our work represents an effort to expand the MLLMs to CAPE. In order to adapt MLLMs into CAPE, we first defined the names and descriptions of keypoints and convert these textual information into an instruction format appropriate to CAPE. Based on the instruction, we set a model architecture to predict category-agnostic keypoint locations. The model includes a visual encoder and a LLM, as shown in Figure 1. Moreover, we investigate the performance variations caused by changes in the instruction and model structures. Consequently, we achieved state-of-the-art results on the MP-100 benchmark, surpassing the 5-shot performance of existing models with a 1-shot framework.

Our contributions can be summarized as follows:

- We introduce CapeLLM, a support image-free CAPE framework with advanced query-text comprehension capabilities, leveraging an MLLM. This work presents the first integration of a mechanism within the CAPE framework to comprehensively understand text query description through the application of MLLM.
- We establish an optimal configuration for instructing the MLLM for CAPE, based on extensive experimental evaluations. This involves curating a comprehensive set of keypoint names and descriptions across all categories, and identifying the most effective configuration of the instruction given these descriptions for CAPE.
- We achieve state-of-the-art results on the MP-100 dataset for CAPE, surpassing the 5-shot accuracy of existing methods [7, 22] with the 1-shot CapeLLM. Table 1 presents a comparative analysis highlighting the advantages of our approach over previous methods.

2. Related Work

2.1. Category-Agnostic Pose Estimation

Category-Agnostic Pose Estimation (CAPE) is a task that aims to estimate the positions of keypoints for object categories not encountered during training [2, 7, 16, 21, 22, 24, 31]. To achieve this, models are trained on data from a variety of categories which have different definition of keypoints on each category, predicting keypoints for new classes. Because the categories in test set are often distinct from train set, in order to guess the locations, previous works [2, 7, 16, 21, 24, 31] have introduced additional support data, provided as pairs consisting of an image from the same category as the query image but with a different appearance, along with its corresponding keypoint annotations. The performance is evaluated as N-shot depending on the number of such pairs supplied.

Approaches tackling CAPE can be broadly divided into two strategies: structural modifications [2, 16, 21, 24, 31]

and changes in the information provided [7, 22]. The simplest structure was first proposed, which predicts keypoint positions by matching support data with the query image [31]. This method connects different pieces of information using cross-attention and outputs similarity scores. While intuitive, it suffers from significant overfitting to the training data. To address this issue, an additional process was introduced to refine the matching results. This enhancement resolves the problems of the previous one-stage architecture and achieves higher performance by reducing dependence on the initial matching outcomes [24]. Keeping the structure similar, performance can also be improved by increasing the amount of provided information. To impart interconnectivity among keypoints rather than treating them as independent entities, skeleton data is incorporated during training [7]. By simply adding connection information, this approach not only achieved better quantitative performance than before but also demonstrated stable results in scenarios like occlusions. Recently, there has been a move to replace the support data used in earlier studies with textual descriptions [22]. Instead of support images and corresponding annotations, “keypoint names” defined for each category are directly created and provided as input to the model. By employing a text encoder [13] trained on image-text similarity, they overcame the limitations of existing support data and achieved results surpassing previous state-of-the-art in 1-shot performance, but still inferior to 5-shot of [7].

In addition to these methods, various approaches have been proposed, such as extracting and utilizing meaningful information from the provided support data [21], or defining meta-points [2, 16] to link keypoints with similar semantics across multiple categories. However, these methods have not solved the fundamental problem that the model’s predictions are dependent on the auxiliary information.

2.2. MLLMs for Visual Localization

Recently, Multimodal Large Language Models (MLLMs) have been surpassing state-of-the-art performance in vision challenges, particularly in traditional localization areas like object detection and segmentation [3, 12, 27–29].

Pix2Seq[3] introduces a novel perspective by transforming conventional object recognition problems into language modeling tasks. By eliminating overly task-specific modules, it streamlines the model architecture and enables language modeling by quantizing bounding boxes into input sequences. VisionLLM[27] leverages Large Language Models (LLMs) to expand predefined vision-centric assignments into open-ended ones. There is also an approach to solve pose estimation problems by utilizing such multimodality [26]. Unlike earlier studies, it predicts coordinates directly from the outputs of existing LLMs without the need to create separate tokens for coordinates.

Going further, some approaches use existing models as

decoders instead of decoding text outputs [12, 28]. They make the outputs of LLMs be suitable for specific applications by employing foundation models in each vision domain [10, 15]. Recently, attempts have emerged to unify models for a variety of vision domains into a single large model[29]. By assigning pre-trained task-specific decoders and training them simultaneously, it achieved high performance not only in visual perception but also in image generation.

With the success of these MLLMs, we became intrigued about whether they can assist in predicting category-agnostic keypoints. Unlike the above challenges addressed in previous research, CAPE has an absolutely small number of samples in benchmark datasets. Conversely, it encompasses a wide array of categories, and there is a substantial domain distribution gap between training and testing. For instance, we might train on the “person” category and evaluate performance on “elephants” during testing. We aim to explore whether these limitations in data aspects can be overcome using MLLMs.

Method	Category-Agnostic	Support-free	LLM-based
GraphCAPE [7]	✓	✗	✗
Capex [22]	✓	✓	✗
Capellm (Ours)	✓	✓	✓

Table 1. Difference between prior methods and ours.

3. Capellm

We propose a novel approach that can reason the location of keypoints which are not seen during training. This approach liberates us from the fluctuation in accuracy caused by support data and eliminates the hassle involved in preparing such information.

3.1. Architecture

Similar to prior works [14, 26], we utilize a pre-trained visual encoder in conjunction with a language model. To extract features across various categories, we adopt DINO-v2 [17], which has been pre-trained on large-scale images with a variety of classes, as our visual encoder. For the language model, we select a LLaMA3.1 [6], which has a powerful capability in wide range of language tasks. The overall architecture is schematically illustrated in Figure 2.

Our goal is to estimate keypoint coordinates of unseen categories only grounded on a query image and a text sequence that contains detailed information about the keypoint. To achieve this, the input image $\mathbf{I} \in \mathbb{R}^{H \times W \times 3}$ is first divided into small patches, where H and W denote height and width of the image, respectively. The patch images are processed through the visual encoder f_ϕ to obtain the patch-processed image features $\tilde{\mathbf{V}} \in \mathbb{R}^{N_v \times C}$, where

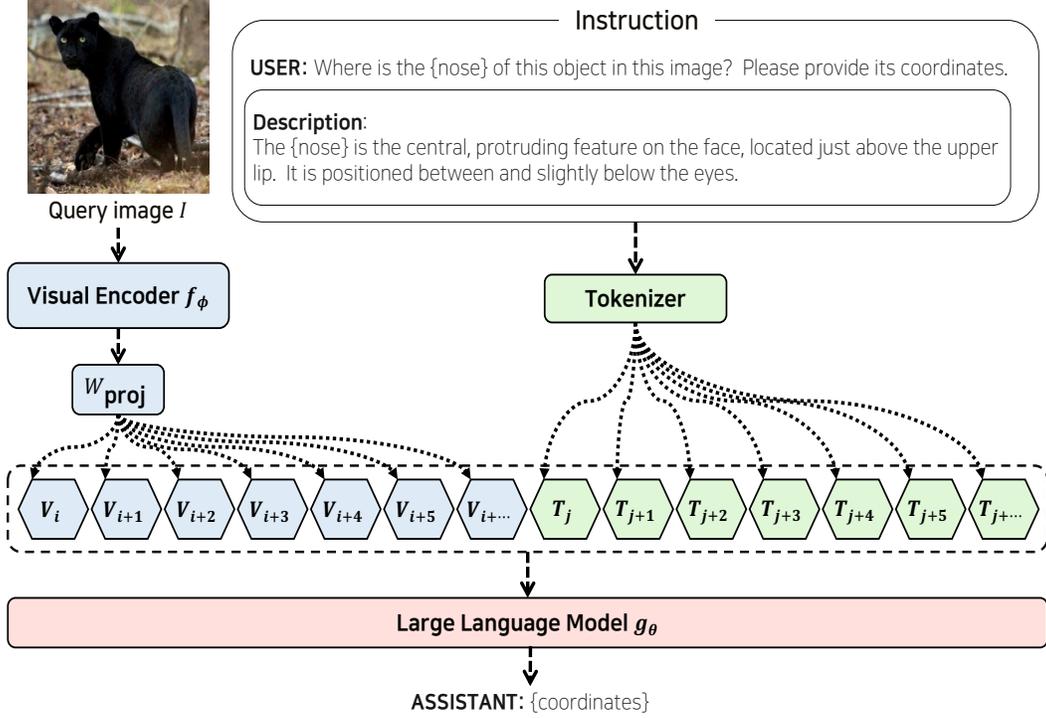


Figure 2. CapeLLM Architecture. CapeLLM consists of two pre-trained modules, visual encoder f_ϕ and LLM g_θ . The query image is transformed to the visual tokens V through the visual encoder f_ϕ and the tokens V are fed into the LLM g_θ with the text tokens T . In this procedure, the projection layer W_{proj} is used to align the visual tokens V with the text tokens T .

N_v is the number of patches and C is the dimension of each patch. These patches are linearly transformed into image tokens $\mathbf{V} \in \mathbb{R}^{N_v \times D}$, via a simple learnable matrix $\mathbf{W}_{\text{proj}} \in \mathbb{R}^{C \times D}$ in Eq (2):

$$\tilde{\mathbf{V}} = f_\phi(\mathbf{I}) \quad (1)$$

$$\mathbf{V} = \tilde{\mathbf{V}}\mathbf{W}_{\text{proj}}, \quad (2)$$

where D represents the dimension of each image token.

These image tokens are prepended to the query text token embeddings $\mathbf{T} \in \mathbb{R}^{N_t \times D}$, where N_t denotes the number of text tokens, and then fed into the language model as the final input tokens $\mathbf{X} \in \mathbb{R}^{N \times D}$:

$$\mathbf{X} = [\mathbf{V}; \mathbf{T}], \quad (3)$$

where $;$ denotes concatenation of the two matrices along the token dimension, and $N = N_v + N_t$.

The decoder-only LLM g_θ processes the input X to produce the output token matrix \mathbf{Z} which has the same shape as \mathbf{X} :

$$\mathbf{Z} = g_\theta(\mathbf{X}). \quad (4)$$

Finally, following previous practices as in [14, 26], a linear transformation with learnable parameters $\mathbf{W}_{\text{logit}} \in$

$\mathbb{R}^{D \times M}$ outputs the final logits $\mathbf{Y} \in \mathbb{R}^{N \times M}$ for each token, where M is the size of the vocabulary:

$$\mathbf{Y} = \mathbf{Z}\mathbf{W}_{\text{logit}}. \quad (5)$$

The response is generated based on the logit with the highest probability.

3.2. Instruction for CAPE

In MLLMs, appropriate instruction is one of the key factors that can affect the model performance [4, 14, 36]. We made the structure of instruction as a format of Visual Question-Answering (VQA) following [14], and modified it to be fitted to the CAPE. As described in Figure 2, the question is filled with the name of keypoint, asking where the keypoint is. Additionally, we provide a reference to help estimate its location. Finally, the model responds with the corresponding keypoint coordinates, considering the above information.

The instruction encompasses the name, description, and positional information of a keypoint. Since the benchmark dataset does not provide keypoint names for all categories, we created keypoint names for each category first. For certain categories, such as the *human face*, keypoints are so densely distributed that it is hard to define them clearly. To clearly distinguish between closely situated keypoints, we

define their names, considering the relative position of keypoints. In the descriptions, relationships with nearby keypoints as well as each position are reflected on them, intentionally avoiding vague expressions. For instance, when describing the “front wheel” of a *swivel chair*, instead of saying “starting from this wheel, the remaining wheels are located clockwise”, we used “next to the fifth wheel and in front of the second wheel” for clarity. Further details on keypoint names and descriptions are discussed in the Appendix A.

Keypoint coordinates are expressed as normalized floating-point values. While various coordinate representation methods have been proposed, such as integer-valued binning [3] and deviation from predefined anchors [18], they come with inconveniences like the need to add numerous new tokens to the vocabulary of LLM or dependence on pre-defined anchors. To maintain a simple structure and refer to the similar prior method [26], we adopt the floating-point coordinate representation. Specifically, we normalize each coordinates to a range of 0 and 1 and construct the ground truth by converting them into text format up to the 3rd decimal place.

3.3. Training Strategy

The training dataset contains images from a variety of categories, each with different numbers and definitions of keypoints. To construct image-instruction pairs for these diverse categories, we group the keypoints(K_c) into fixed units of size k first, where K_c denotes the number of keypoints in category c . This approach is similar to the multi-round conversation [26], but different in that we allow image duplication. Instead of a single image only with some k keypoints in an epoch, we permit image repetition until all keypoints have been paired. Let’s consider an example of the category *bird*. The category has 15 keypoints($K_{bird}=15$). If we set $k=5$, three pairs are generated for a single image of *bird*, 5 keypoints in a pair. If the total number of keypoints is not divisible by k , we randomly sample the remaining keypoints from the entire keypoints to make a complete pair. This ensures that no keypoints are omitted during training for any single image.

To ensure efficient training, we organized the instructions in a multi-round conversation format, which means that an instruction is made up multiple QA samples, where each QA sample is about a keypoint, as shown in Figure 2. Unlike prior work [26] and as mentioned right above, we made the pairs for all keypoints, allowing the duplication of image. So, we can build the training dataset where total examples are over 60,000 for most of splits in MP-100 and each example turn into the k -round conversation as a model input.

4. Experiment

4.1. Benchmark

We utilize the MP-100 benchmark dataset [31], aligning with prior methods [2, 7, 16, 21, 22, 24, 31]. MP-100 comprises 100 categories and approximately 20,000 images. These categories are split into train, validation, and test sets in a 70/10/20 ratio without any category overlap. To ensure and identify performance stability on unseen categories, it consists of five different splits, carefully arranging for each category to appear once in the test set. The number of keypoints per category varies significantly, ranging from 8 to 68. We discovered that in some categories (e.g., “hand”), images did not correctly correspond to keypoints; we rectified these discrepancies before proceeding with experiments. We use PCK@0.2 as a measurement of accuracy and compare both quantitative and qualitative results with two models as representatives: GraphCAPE [7] and CapeX [22]. GraphCAPE [7] holds the highest 1-shot and 5-shot accuracy among models employing a query-support paired architecture(as seen in upper side of Figure 1). CapeX [22], based on the GraphCAPE framework, is text-based query architecture utilizing keypoint names instead of support data. It demonstrated higher 1-shot performance than GraphCAPE [7] by connecting text features extracted via a text encoder[13] to image features. Because of their overwhelmingly superior performance compared to other models, both quantitatively and qualitatively, we set these two methods as our baseline.

4.2. Implementation Details

The model architecture consists of a visual encoder, a projection layer, and an LLM. We choose DINO-v2 [17] as our vision encoder. Inspired by [14], the projection layer linking the vision and the text part is implemented as a linear layer. For the base language model, we use the pre-trained decoder-only model, LLaMA-3.1 [6]. To fully leverage the capabilities of large-scale pre-trained models and adjust them to this task, we employ LoRA [8]. Following the setting of [26], we applied it to the query/value projection of the attention layers in both the visual encoder and the LLM, projecting them into the dimension of a rank 8. Additionally, following a previous work [26], we selected AdamW as the optimizer and set the learning rate to 5×10^{-4} . The total number of training epochs was set to 12, with a warm-up phase over 3% of the total training steps. Input images were resized to 224×224 pixels, and the default number of rounds included in each instruction was set to 4. Training was conducted on a Linux server equipped with four RTX-A6000 GPUs; instead of setting the batch size to 1 per GPU, we set the accumulation steps to 32.

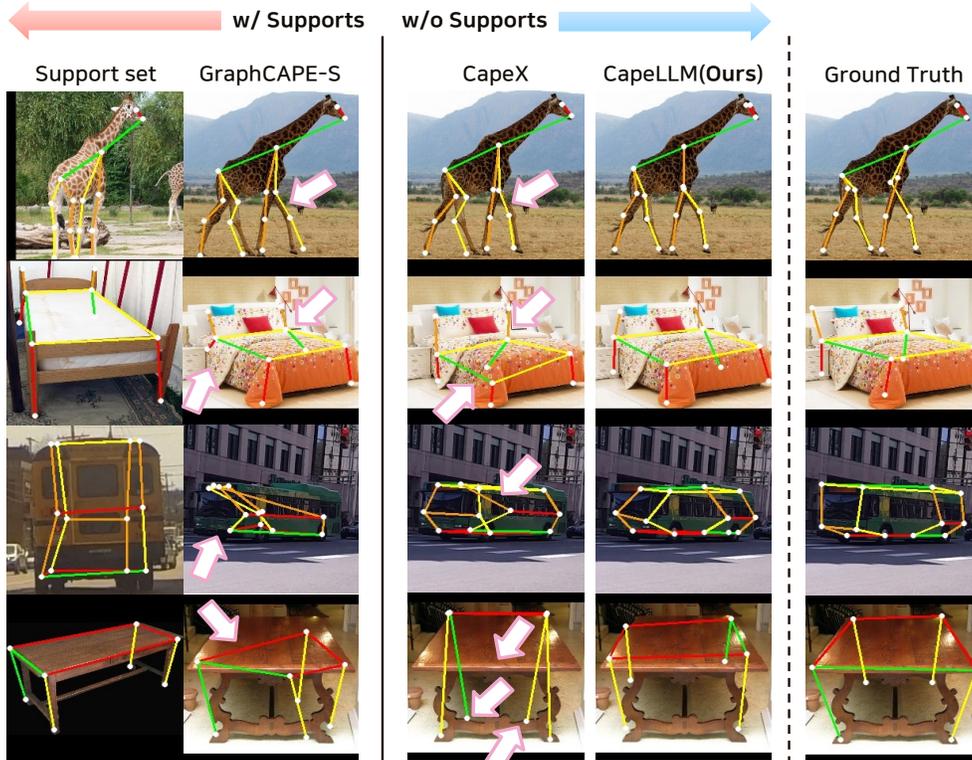


Figure 3. Qualitative results on MP-100. The support set is only used for GraphCAPE [7]

Evaluation dataset	Model	split1	split2	split3	split4	split5	Avg
Support-Query Pairs	GraphCAPE-S(1-shot) [7]	94.63	89.79	90.30	87.81	90.07	90.52
	GraphCAPE-S(5-shot) [7]	95.81	90.78	90.94	90.42	92.27	92.04
	CapeX [22]	95.29	91.08	88.94	89.83	92.96	91.62
	CapeLLM (Ours)	97.01	92.40	90.58	90.90	92.11	92.60
Only Query Images	CapeX [22]	95.28	91.08	89.06	89.67	92.87	91.59
	CapeLLM (Ours)	96.98	92.34	90.57	90.87	92.24	91.60

Table 2. PCK@0.2 on the MP-100 dataset.

4.3. Benchmark Results

Quantitative Results GraphCAPE [7] configures the test dataset with support-query pairs, but our model is support-free method, not considering the supports at all. For fair comparison, we made the same test set with GraphCAPE [7] and measured the performance on the test set (“Support-Query Pairs”). We surpassed the 1-shot accuracy of this model over 1%p and further achieved 0.56%p higher accuracy than its 5-shot performance, as demonstrated in Table 2. Note that the information provided for 5-shot CAPE is strictly larger than in our case. Remarkably, this demonstrates that even without any support, it is possible to attain superior results in CAPE. We also compared our model with CapeX [22] using about 2,000 query

images from each split (“Only Query Images”) in Table 2. Achieving almost 1%p higher accuracy than the model using sequences of keypoint names as input, we accomplished a new state-of-the-art in CAPE.

Qualitative Results As can be seen in Figure 3, we demonstrate that our CapeLLM is superior to conventional methods across various categories. Specifically, in *animal body*, remarkable improvements have been found in end joints, such as knees and paws, which the preceding approaches [7, 22] have struggled to predict. In other categories, prior methods [7, 22] showed imprecise results; for example, GraphCAPE [7] failed to estimate due to differences of pose in the supports, and CapeX [22] confused the front and rear joints. Our method, however, produced more



Figure 4. Effect of different keypoint names in *animal body*. The left side above is the basic definition of *animal body*, and the opposite side is the re-generated definition by ChatGPT-4o; the colored ones mean the names altered. As a result, there is no critical difference in coordinates.

accurate results, working as intended based on the given instructions, and outperforming previous approaches [7, 22].

4.4. Ablation Study

Since our work is the first attempt to introduce MLLM into this task, It is necessary to systematically examine how the configurations of instructions and model architecture affect performance. Accordingly, subsequent experiments aim to contribute to establishing the better model structure by conducting ablation studies to assess the suitability of various components in carrying out category-agnostic keypoint estimation. We expect that our ablations provide meaningful insights for utilizing MLLMs in CAPE. The ablation results were conducted on the test set of split1.

Instruction As mentioned in Sec 3.2, we included not only the names but also descriptions of the keypoints in the instructions to help the model better reason the keypoint’s location. We examined test results between models with and without descriptions to confirm how the descriptions affected model performance. The result in Table 3 showed that adding the descriptions made the model be improved by 0.76%p. This suggests that keypoint descriptions play a significant role in enhancing to find the accurate location. Additionally, we conducted extra experiments to increase the amount of information by including the list of keypoints defined for the category. As shown in Table 3, unlike keypoint descriptions, the list of keypoint names as an additional information is not helpful for the model to improve

in inferring the position of the keypoint, rather reducing the performance. Lastly, we investigated the optimal number of rounds k in the conversation (Table 4). Here, the rounds refer to number of instruction iterations to infer the keypoints for one query image. Experimented under the same training conditions, the highest performance was observed when k was set to 4. No explicit tendency was found as k changed. As a result, while keypoint descriptions are an important factor strengthening the performance, adding fixed and iterative information seems to be redundant and to cause confusion for the model when performing CAPE. Additional experiments related to instructions can be found in the Appendix B.1.

Visual Encoder While some exceptions exist [26], most of MLLM-related researches tended to train the model with the visual encoder frozen [14, 27, 29, 36]. To demonstrate that this convention also works in CAPE, we tested three cases about visual encoder with different setting, frozen, parameter efficient tuning with LoRA [8], and fine-tuning on all parameters. The experimental results in the second row of Table 4 show that tuning the visual encoder with LoRA was more advantageous than the other two options. Notably, the full fine-tuning approach, where all parameters are trained, significantly degraded performance. This imply that leaving all parameters trainable may lead to overfitting and thus result in performance degradation in the tasks using relatively small datasets. Next, we examined the drop-in-replacement effect in visual encoder. We se-

w/ description	w/ keypoint list	PCK@0.05	PCK@0.1	PCK@0.15	PCK@0.2	PCK@0.25	mPCK
×	×	72.60	89.02	94.02	96.22	97.44	89.86
✓	×	78.43	91.34	95.26	96.98	97.90	91.98
✓	✓	77.36	90.72	94.28	95.80	96.67	90.97

Table 3. Effect of adding descriptive information to the instruction.

Ablations	Conditions	PCK@0.05	PCK@0.1	PCK@0.15	PCK@0.2	PCK@0.25	mPCK
Multi-round k	$k = 1$	78.29	91.55	95.19	96.89	97.88	91.96
	$k = 2$	72.82	88.06	92.79	95.30	96.56	89.11
	$k = 4$	78.43	91.34	95.26	96.98	97.90	91.98
	$k = 6$	74.33	89.82	94.17	96.36	97.46	90.43
	$k = 8$	75.28	89.89	93.99	96.16	97.41	90.55
Visual encoder fine-tuning	None (Frozen)	69.69	88.16	92.62	95.07	96.41	88.39
	LoRA [8]	78.43	91.34	95.26	96.98	97.90	91.98
	Full parameters	6.93	23.72	42.41	55.31	64.56	38.59
Visual encoder model	DINO-v2 [17]	78.43	91.34	95.26	96.98	97.90	91.98
	DINO-v2-reg [5]	62.52	86.00	92.83	95.83	97.34	86.90
	Hiera [23]	56.13	83.31	91.99	95.67	97.35	84.89
LLM	Llama3.2-1B [1]	76.46	91.05	94.69	96.41	97.40	91.20
	Vicuna-7B-v1.5 [35]	62.15	84.40	91.51	94.79	96.33	85.84
	Mistral-7B-v0.3 [9]	77.63	91.32	94.90	96.46	97.54	91.57
	Llama3.1-8B [6]	78.43	91.34	95.26	96.98	97.90	91.98

Table 4. MP-100 results on different ablations.

lected three types of visual encoders [5, 17, 23] pre-trained on same dataset and compared them. The results in Table 4 showed that using DINOv2 [17] yielded the highest performance. Structural issues observed during pre-training (e.g., artifacts in the feature maps [5]) did not have a significant impact on performance in the CAPE task. A particularly noteworthy point is the number of image tokens. Although Hiera [23] have less than 20% of the image tokens compared to the other two encoders, the performance gap is less than about 1%, implying that retaining a larger number of image tokens does not necessarily have a significant impact on performance.

LLM To analyze the variations in model performance across different LLMs, we experimented on four language models [1, 6, 9, 35]. Generally, we observed that the overall accuracy improved as the size of the LLM increased (last row of Table 4). Exceptionally, Llama3.2-1B [1] exhibited performance surpassing that of a 7B-sized LLM, Vicuna-7B-v1.5, which appears to be the result of effectively transferring the knowledge of a larger model through distillation training methods. We expect that a larger vocabulary size might also play a crucial role to positively influence the integration of visual information and language. More experimental findings for finding the better architecture are provided in Appendix B.2.

Different Keypoint Names We investigated that whether the changes in keypoint names of an category affects the model prediction. To do this, we chose the category, *animal body*, which contains the most various sub-categories, such as dog, fox and horse. We changed its keypoint definitions using most frequently used and closed-source model, ChatGPT-4o, prompting them to generate the similar meaning but different expression. The corresponding descriptions are adapted only for the changed parts. As shown in Figure 4, no significant degradation of the prediction performance is observed, finding out the correct position of each keypoint in the image irrespective of the keypoint name.

5. Discussion and Conclusion

We introduce CapeLLM, a novel approach for estimating category-agnostic keypoints without reliance on support image-keypoint pairs, as required by conventional methods. Our architecture integrates a visual encoder with a language model pretrained on large-scale data, leveraging the reasoning capabilities of a LLM. Instead of the support pairs, we define a comprehensive set of keypoint names and corresponding descriptions for each category, constructing instruction-based training with query image data. As a result, 1-shot CapeLLM achieves state-of-the-art performance on the CAPE benchmark, surpassing both 1-shot and 5-shot accuracies of previous methods.

References

- [1] Meta AI. Llama 3.2: Vision Edge for Mobile Devices, 2024. <https://ai.meta.com/blog/llama-3-2-connect-2024-vision-edge-mobile-devices/>. 8, 13
- [2] Junjie Chen, Jiebin Yan, Yuming Fang, and Li Niu. Meta-Point Learning and Refining for Category-Agnostic Pose Estimation. In *Proceedings of the IEEE/CVF Conference on Computer Vision and Pattern Recognition*, pages 23534–23543, 2024. 1, 2, 3, 5
- [3] Ting Chen, Saurabh Saxena, Lala Li, David J. Fleet, and Geoffrey Hinton. Pix2seq: A Language Modeling Framework for Object Detection. In *International Conference on Learning Representations*, 2022. 3, 5
- [4] Wenliang Dai, Junnan Li, Dongxu Li, Anthony Tiong, Junqi Zhao, Weisheng Wang, Boyang Li, Pascale Fung, and Steven Hoi. InstructBLIP: Towards General-purpose Vision-Language Models with Instruction Tuning. In *Thirty-seventh Conference on Neural Information Processing Systems*, 2023. 4
- [5] Timothée Darcet, Maxime Oquab, Julien Mairal, and Piotr Bojanowski. Vision Transformers Need Registers. In *The Twelfth International Conference on Learning Representations*, 2024. 8
- [6] Abhimanyu Dubey, Abhinav Jauhri, Abhinav Pandey, Abhishek Kadian, Ahmad Al-Dahle, Aiesha Letman, Akhil Mathur, Alan Schelten, Amy Yang, Angela Fan, et al. The llama 3 herd of models. *arXiv preprint arXiv:2407.21783*, 2024. 3, 5, 8, 13
- [7] Or Hirschorn and Shai Avidan. A graph-based approach for category-agnostic pose estimation, 2024. 1, 2, 3, 5, 6, 7
- [8] Edward J Hu, Yelong Shen, Phillip Wallis, Zeyuan Allen-Zhu, Yuanzhi Li, Shean Wang, Lu Wang, and Weizhu Chen. LoRA: Low-Rank Adaptation of Large Language Models. In *International Conference on Learning Representations*, 2022. 5, 7, 8
- [9] Albert Q Jiang, Alexandre Sablayrolles, Arthur Mensch, Chris Bamford, Devendra Singh Chaplot, Diego de las Casas, Florian Bressand, Gianna Lengyel, Guillaume Lample, Lucile Saulnier, et al. Mistral 7B. *arXiv preprint arXiv:2310.06825*, 2023. 8
- [10] Alexander Kirillov, Eric Mintun, Nikhila Ravi, Hanzi Mao, Chloe Rolland, Laura Gustafson, Tete Xiao, Spencer Whitehead, Alexander C Berg, Wan-Yen Lo, et al. Segment anything. In *Proceedings of the IEEE/CVF International Conference on Computer Vision*, pages 4015–4026, 2023. 3
- [11] Rollyn Labuguen, Jumpei Matsumoto, Salvador Blanco Negrete, Hiroshi Nishimaru, Hisao Nishijo, Masahiko Takada, Yasuhiro Go, Ken-ichi Inoue, and Tomohiro Shibata. MacaquePose: a novel “in the wild” macaque monkey pose dataset for markerless motion capture. *Frontiers in behavioral neuroscience*, 14:581154, 2021. 1
- [12] Xin Lai, Zhuotao Tian, Yukang Chen, Yanwei Li, Yuhui Yuan, Shu Liu, and Jiaya Jia. Lisa: Reasoning segmentation via large language model. In *Proceedings of the IEEE/CVF Conference on Computer Vision and Pattern Recognition*, pages 9579–9589, 2024. 2, 3, 11
- [13] Zehan Li, Xin Zhang, Yanzhao Zhang, Dingkun Long, Pengjun Xie, and Meishan Zhang. Towards general text embeddings with multi-stage contrastive learning. *arXiv preprint arXiv:2308.03281*, 2023. 3, 5
- [14] Haotian Liu, Chunyuan Li, Qingyang Wu, and Yong Jae Lee. Visual instruction tuning. *Advances in neural information processing systems*, 36, 2024. 2, 3, 4, 5, 7
- [15] Shilong Liu, Zhaoyang Zeng, Tianhe Ren, Feng Li, Hao Zhang, Jie Yang, Chunyuan Li, Jianwei Yang, Hang Su, Jun Zhu, et al. Grounding dino: Marrying dino with grounded pre-training for open-set object detection. *arXiv preprint arXiv:2303.05499*, 2023. 3
- [16] Khoi Duc Nguyen, Chen Li, and Gim Hee Lee. ESCAPE: Encoding Super-keypoints for Category-Agnostic Pose Estimation. In *Proceedings of the IEEE/CVF Conference on Computer Vision and Pattern Recognition*, pages 23491–23500, 2024. 1, 2, 3, 5
- [17] Maxime Oquab, Timothée Darcet, Théo Moutakanni, Huy V. Vo, Marc Szafraniec, Vasil Khalidov, Pierre Fernandez, Daniel HAZIZA, Francisco Massa, Alaaeldin El-Nouby, Mido Assran, Nicolas Ballas, Wojciech Galuba, Russell Howes, Po-Yao Huang, Shang-Wen Li, Ishan Misra, Michael Rabbat, Vasu Sharma, Gabriel Synnaeve, Hu Xu, Herve Jegou, Julien Mairal, Patrick Labatut, Armand Joulin, and Piotr Bojanowski. DINOv2: Learning Robust Visual Features without Supervision. *Transactions on Machine Learning Research*, 2024. 3, 5, 8
- [18] Kanchana Ranasinghe, Satya Narayan Shukla, Omid Pour-saeed, Michael S Ryoo, and Tsung-Yu Lin. Learning to localize objects improves spatial reasoning in visual-llms. In *Proceedings of the IEEE/CVF Conference on Computer Vision and Pattern Recognition*, pages 12977–12987, 2024. 5, 11
- [19] N Dinesh Reddy, Minh Vo, and Srinivasa G Narasimhan. Carfusion: Combining point tracking and part detection for dynamic 3d reconstruction of vehicles. In *Proceedings of the IEEE conference on computer vision and pattern recognition*, pages 1906–1915, 2018. 1
- [20] N Dinesh Reddy, Minh Vo, and Srinivasa G Narasimhan. Occlusion-net: 2d/3d occluded keypoint localization using graph networks. In *Proceedings of the IEEE/CVF conference on computer vision and pattern recognition*, pages 7326–7335, 2019. 1
- [21] Pengfei Ren, Yuanyuan Gao, Haifeng Sun, Qi Qi, Jingyu Wang, and Jianxin Liao. Dynamic Support Information Mining for Category-Agnostic Pose Estimation. In *Proceedings of the IEEE/CVF Conference on Computer Vision and Pattern Recognition*, pages 1921–1930, 2024. 1, 2, 3, 5
- [22] Matan Rusanovsky, Or Hirschorn, and Shai Avidan. CapeX: Category-Agnostic Pose Estimation from Textual Point Explanation. *arXiv preprint arXiv:2406.00384*, 2024. 1, 2, 3, 5, 6, 7
- [23] Chaitanya Ryali, Yuan-Ting Hu, Daniel Bolya, Chen Wei, Haoqi Fan, Po-Yao Huang, Vaibhav Aggarwal, Arkabandhu Chowdhury, Omid Poursaeed, Judy Hoffman, et al. Hiera: A hierarchical vision transformer without the bells-and-whistles. In *International Conference on Machine Learning*, pages 29441–29454. PMLR, 2023. 8

- [24] Min Shi, Zihao Huang, Xianzheng Ma, Xiaowei Hu, and Zhiguo Cao. Matching is not enough: A two-stage framework for category-agnostic pose estimation. In *Proceedings of the IEEE/CVF Conference on Computer Vision and Pattern Recognition*, pages 7308–7317, 2023. 1, 2, 3, 5
- [25] Ke Sun, Bin Xiao, Dong Liu, and Jingdong Wang. Deep high-resolution representation learning for human pose estimation. In *Proceedings of the IEEE/CVF conference on computer vision and pattern recognition*, pages 5693–5703, 2019. 1
- [26] Dongkai Wang, Shiyu Xuan, and Shiliang Zhang. LocLLM: Exploiting Generalizable Human Keypoint Localization via Large Language Model. In *Proceedings of the IEEE/CVF Conference on Computer Vision and Pattern Recognition*, pages 614–623, 2024. 3, 4, 5, 7, 11
- [27] Wenhai Wang, Zhe Chen, Xiaokang Chen, Jiannan Wu, Xizhou Zhu, Gang Zeng, Ping Luo, Tong Lu, Jie Zhou, Yu Qiao, et al. Visionllm: Large language model is also an open-ended decoder for vision-centric tasks. *Advances in Neural Information Processing Systems*, 36, 2024. 2, 3, 7, 11
- [28] Fei Wei, Xinyu Zhang, Ailing Zhang, Bo Zhang, and Xi-angxiang Chu. Lenna: Language enhanced reasoning detection assistant. *arXiv preprint arXiv:2312.02433*, 2023. 3, 11
- [29] Jiannan Wu, Muyan Zhong, Sen Xing, Zeqiang Lai, Zhaoyang Liu, Zhe Chen, Wenhai Wang, Xizhou Zhu, Lewei Lu, Tong Lu, Ping Luo, Yu Qiao, and Jifeng Dai. Vision-LLM v2: An End-to-End Generalist Multimodal Large Language Model for Hundreds of Vision-Language Tasks. In *The Thirty-eighth Annual Conference on Neural Information Processing Systems*, 2024. 2, 3, 7, 11
- [30] Bin Xiao, Haiping Wu, and Yichen Wei. Simple baselines for human pose estimation and tracking. In *Proceedings of the European conference on computer vision (ECCV)*, pages 466–481, 2018. 1
- [31] Lumin Xu, Sheng Jin, Wang Zeng, Wentao Liu, Chen Qian, Wanli Ouyang, Ping Luo, and Xiaogang Wang. Pose for everything: Towards category-agnostic pose estimation. In *European conference on computer vision*, pages 398–416. Springer, 2022. 1, 2, 3, 5
- [32] Yufei Xu, Jing Zhang, Qiming Zhang, and Dacheng Tao. Vit-pose: Simple vision transformer baselines for human pose estimation. *Advances in Neural Information Processing Systems*, 35:38571–38584, 2022. 1
- [33] Hang Yu, Yufei Xu, Jing Zhang, Wei Zhao, Ziyu Guan, and Dacheng Tao. AP-10K: A Benchmark for Animal Pose Estimation in the Wild. In *Thirty-fifth Conference on Neural Information Processing Systems Datasets and Benchmarks Track (Round 2)*, 2021. 1
- [34] Beichen Zhang, Pan Zhang, Xiaoyi Dong, Yuhang Zang, and Jiaqi Wang. Long-clip: Unlocking the long-text capability of clip. In *European Conference on Computer Vision*, pages 310–325. Springer, 2025. 2
- [35] Lianmin Zheng, Wei-Lin Chiang, Ying Sheng, Siyuan Zhuang, Zhanghao Wu, Yonghao Zhuang, Zi Lin, Zhuohan Li, Dacheng Li, Eric Xing, et al. Judging llm-as-a-judge with mt-bench and chatbot arena. *Advances in Neural Information Processing Systems*, 36:46595–46623, 2023. 8
- [36] Deyao Zhu, Jun Chen, Xiaoqian Shen, Xiang Li, and Mohamed Elhoseiny. MiniGPT-4: Enhancing Vision-Language Understanding with Advanced Large Language Models. In *The Twelfth International Conference on Learning Representations*, 2024. 4, 7

CapeLLM: Support-Free Category-Agnostic Pose Estimation with Multimodal Large Language Models

Supplementary Material

A. Keypoint Descriptions

We created the names and descriptions of keypoints for all 100 categories. The names can be divided into two types: the one that has its own unique name, e.g., “left shoulder”, “right eye”, and the other that does not have its own name and is difficult to define due to the densely distributed position. We concentrate on designating the latter and determine the names using their relative positions in each category; for example, “upper”, “central”, “lower”. The descriptions are represented with the keypoint position in the category and its relationship with other keypoints; e.g., in the *animal body* category, the description of “left front paw” is defined as “The left front paw is the lower end of the left forelimb, used for movement and manipulation of objects. It is positioned below the left elbow and connected with the left elbow”. A detailed example can be found in Table 5.

B. Exploring other Design Choices

B.1. Instruction

We conducted two additional experiments regarding the way instructions are structured. First, we experimented with increasing the amount of information provided, such as adding a conversation outline and diversifying question expressions. The outline consists of what the task is and how the conversation flows. And we made a list of questions that have the same meaning but different expressions by employing ChatGPT-4o and randomly picked up the one from the list in training. In contrast to keypoint descriptions (Figure 3), this approach of adding the outline that is fixed in training and randomizing the questions did not help improve the model and actually led to decreased performance, as in Table 6.

Next, we restructured the instruction to progress QA in a step-by-step manner, so-called *step-by-step instruction*. Specifically, instead of directly providing keypoint descriptions and estimating coordinates as in Figure 2, we first asked about the object and then inquired about the keypoints (Figure 5). We expected this approach would help the model better understand the input information. When we compared the performance to verify this hypothesis, the effect varied depending on the LLM, as in Table 7. It appears that different LLMs require different approaches to providing information for better understanding of input data.

B.2. Architecture

We explored a method that utilizes token embeddings `<KEYPOINT>` instead of text-based outputs. To apply this approach to our pipeline, some modifications in instruction should be made: the coordinates are replaced with special token `<KEYPOINT>` as answers, accordingly the vocabulary size increases, and input embeddings are turned into the trainables. The tokens are turned into the output embeddings from the LLM and are fed into a task-specific decoder. Typically, a grounding-based pre-trained decoder [12, 28, 29] is used; however, since no similar model exists for pose estimation, we created a simple decoder that yields the coordinates from the embeddings and trained it from scratch.

As shown in Table 8, we validated this method on the step-by-step instruction as described in Appendix B.1 as well as the base instruction as Figure 2. Despite the lack of pre-training, it achieved performance comparable to models based on text outputs.

C. Training Strategy

Referring to the related works [18, 27, 29] that deal with pre-training techniques on the visual localization tasks, we tried the pre-training on CAPE. The visual encoder and LLM are frozen, and the projection layer is only trainable in the pre-training stage. All data in pre-training is only from the MP-100 dataset. After pre-training, we take the pre-trained weights on the projection layer and carry out the fine-tuning stage with the same setting in Sec 4.2.

Two types of pre-training are attempted: direct QA and step-by-step QA. The direct QA has an instruction that it is in the form of asking and answering the name of the keypoint corresponding to the coordinates, as in Figure 6. On the other hand, step-by-step QA in Figure 7 has an instruction that is in the form of asking about the category, inquiring the existence of the keypoint in the image, and then inducing the selection of the keypoint corresponding to the coordinates. As a consequence, there is no positive effect on the performance gain, as shown in Table 9. In light of the use of large-scale pre-training data in the previous methods [18, 26, 27, 29], we conjecture that the limited number of images in each category might result in this outcome.

Keypoint	Description
Left eye	The left eye is one of the two visual organs located on the face. It is positioned slightly to the left of the nose and just below the brow ridge, visible from the front.
Right eye	The right eye is the visual organ located on the right side of the face. It is situated to the right of the nose and directly opposite the left eye.
Nose	The nose is the central, protruding feature on the face, located just above the upper lip. It is positioned between and slightly below the eyes
Neck	The neck is the part of the body connecting the head to the torso that refers to the area from the shoulders to the hip joints. It is located below the head, near the junction where the shoulders meet the body.
Root of tail	The root of the tail is at the base of the spine, where the tail begins. It is located near the lower back, above the hips.
Left shoulder	The left shoulder is the joint connecting the left arm to the torso. It is situated to the left of the neck and above the left elbow.
Left elbow	The left elbow is the joint in the middle of the left arm, connecting the upper arm to the forearm. It is located between the left shoulder and the left front paw and connectd with them.
Left front paw	The left front paw is the lower end of the left forelimb, used for movement and manipulation of objects. It is positioned below the left elbow and connected with the left elbow.
Right shoulder	The right shoulder is the joint connecting the right arm to the torso. It is located to the right of the neck and above the right elbow.
Right elbow	The right elbow is the joint in the middle of the right arm, connecting the upper arm to the forearm. It is situated between the right shoulder and the right front paw and connectd with them.
Right front paw	The right front paw is the lower end of the right forelimb, used for movement and manipulation of objects. It is located below the right elbow and connectd with the right elbow.
Left hip	The left hip is the joint connecting the left leg to the torso. It is positioned below the root of the tail and above the left knee.
Left knee	The left knee is the joint in the middle of the left leg, connecting the upper leg to the lower leg. It is located between the left hip and the left back paw and connectd with them..
Left back paw	The left back paw is the lower end of the left hind limb, used for movement and support. It is situated below the left knee.
Right hip	The right hip is the joint connecting the right leg to the torso. It is positioned below the root of the tail and above the right knee.
Right knee	The right knee is the joint in the middle of the right leg, connecting the upper leg to the lower leg. It is located between the right hip and the right back paw and connectd with them.
Right back paw	The right back paw is the lower end of the right hind limb, used for movement and support. It is situated below the right knee.

Table 5. An example of descriptions: *animal body*

Diverse questions	Add conversation outline	PCK@0.05	PCK@0.1	PCK@0.15	PCK@0.2	PCK@0.25	mPCK
×	×	78.43	91.34	95.26	96.98	97.90	91.98
✓	×	74.24	89.82	94.45	96.56	97.74	90.56
×	✓	75.08	90.02	94.14	96.27	97.66	90.63
✓	✓	68.24	87.63	93.32	95.93	97.49	88.52

Table 6. Effect of adding a conversation outline and diversifying question expressions.

LLM	Step-by-step instruction	PCK@0.05	PCK@0.1	PCK@0.15	PCK@0.2	PCK@0.25	mPCK
Llama3.1-8B [6]	×	78.43	91.34	95.26	96.98	97.90	91.98
	✓	76.06	90.74	94.62	96.48	97.63	91.11
Llama3.2-1B [1]	×	76.46	91.05	94.69	96.41	97.40	91.20
	✓	76.65	91.13	95.02	96.75	97.88	91.49

Table 7. Performance comparison with *step-by-step instruction* across different LLMs.

Instruction	Output format	PCK@0.05	PCK@0.1	PCK@0.15	PCK@0.2	PCK@0.25	mPCK
Base instruction	text	78.43	91.34	95.26	96.98	97.90	91.98
	special token	76.06	90.74	94.62	96.48	97.63	91.11
Step-by-step instruction	text	76.46	91.05	94.69	96.41	97.40	91.20
	special token	76.65	91.13	95.02	96.75	97.88	91.49

Table 8. Performance comparison in model output format.

USER: What do you think is the central object in this image?

ASSISTANT: The object that this image is trying to express seems to be a {category name}.

USER: Can you identify location of {nose} on the object? The {nose} is the central, protruding feature on the face, located just above the upper lip. It is positioned between and slightly below the eyes. With this description, please provide its coordinates.

ASSISTANT: {coordinates}

Figure 5. Step-by-step instruction. The nose is in the example above, which can be replaced with whatever you want to find out. The underlined is the description of nose, which can also be replaced according to the keypoint.

USER: What is the name of a keypoint at [0.123,0.456] in the image? Tell me the name and why.

ASSISTANT: The keypoint name is nose, because the nose is the central, protruding feature on the face, located just above the upper lip. It is positioned between and slightly below the eyes.

Figure 6. Instruction of direct QA for pre-training.

Training Strategy	PCK@0.05	PCK@0.1	PCK@0.15	PCK@0.2	PCK@0.25	mPCK
w/o pre-training	78.43	91.34	95.26	96.98	97.90	91.98
Direct QA	78.98	91.57	94.96	96.60	97.70	91.96
Step-by-step QA	78.05	90.85	94.51	96.23	97.35	91.40

Table 9. Performance comparison of different training strategies

Joint list: nose, left eye, right eye, ...

USER: What do you think is the central object in this image?

ASSISTANT: The object that this image is trying to express seems to be a {human body}.

USER: What joints can you identify on the {human body} in the image? Answer according to the order in the joint list.

ASSISTANT: The {human body} in the image seems to have several joints in the list, named {nose, left eye, right eye}. Those joints are visible in the image.

USER: Can you identify which joint is located at the coordinate {location}? This coordinate represent relative position within the image, where the top-left corner is defined as [0, 0] and the bottom-right corner as [1, 1]. For example, [0.5, 0.5] indicates the center of the image

ASSISTANT: the joint located at coordinates is {left eye}.

Figure 7. Instruction of step-by-step QA for pre-training.